Earthquake Engineering, Tenth World Conference © 1992 Balkema, Rotterdam. ISBN 90 5410 060 5

# Seismic analysis of nonlinear soil-structure interaction systems using a hybrid experiment

K.Toki & J.Kiyono
*Disaster Prevention Research Institute, Kyoto University, Japan*

ABSTRACT: We here report a hybrid procedure for testing a nonlinear soil-structure interaction system developed from the Pseudo-Dynamic Testing (PDT) method modified to take into account the frequency dependency of complex stiffness. Four large scale 1-, 2-, 3- and 9-pile foundation models were used. For the investigation of the effect of increasing dead loading on the sway-rocking response of pile foundations, the 3-pile group model was used. Four dead loadings of 10, 20, 30 and 40 tons were applied to increase the axial loads on the piles. Seismic data for pile foundations were provided when an earthquake occurred at the experiment site.

## 1 INTRODUCTION

Recently, we developed a hybrid method for the study of seismic, nonlinear soil-pile interaction (Toki 1990). Taking advantage of analytical idealization, the time domain numerical integration scheme, large scale modeling and Pseudo-Dynamic Testing (PDT), we developed an algorithm with which to study the seismic nonlinear behavior of pile-group soil-structure systems.

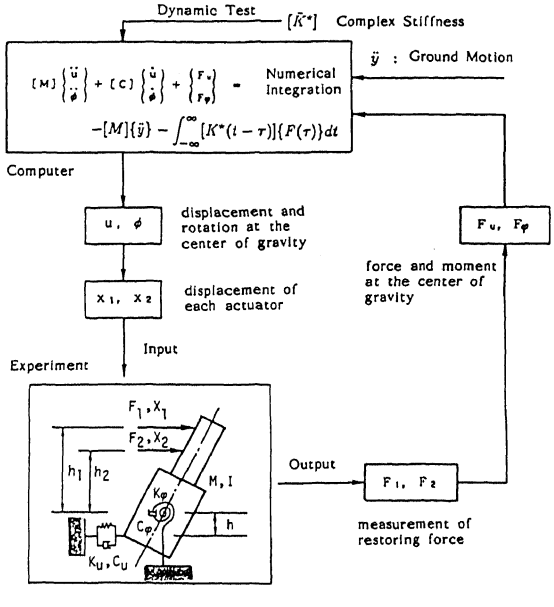


Figure 1. The HENESSI procedure.

Our procedure, a flow-chart for which is shown in Figure 1, is called HENESSI; Hybrid Experiments on Nonlinear Earthquake-induced Soil-Structure Interaction. The procedure starts with large scale modeling after mathematical discretization. Static and forced vibration dynamic tests then are made, from which the mechanical characteristics of the system can be determined. Using these results, we developed a complex frequency-dependent stiffness matrix for the system in the frequency domain. We then used the Hilbert (Papoulis 1962) and inverse Fourier transformations to establish a time-dependent pseudo-force to decompose the equations of motion in terms of the initial, nonlinear and frequency-dependent characteristics of the system. This newly developed scheme was introduced to a PDT algorithm, the results of which we arranged, generalized and studied. On the assumption that inertial interaction effects are, in general, more important than kinematic ones (Veletsos 1988), we neglected the low-pass filtering effect of the kinematic interaction.

## 2 HYBRID EXPERIMENT

### 2.1 Test set-up and modeling

We used single, 2-, 3- and 9-pile group foundation models (PL1, PL2, PL3 and PL9), shown schematically in Figure 2. The pile spacings were set according to the Japanese seismic design code to minimize the pile group effects. Table 1 shows the geometric and mechanical properties of the foundations. Six-meter-long steel piles, whose properties are shown in Table 2, were driven into a soil deposit whose upper three meters had been replaced by fine-grained sand.

For the foundations, relatively rigid concrete super-structures were constructed to maintain the dead-weight and to transmit the forces applied by the actuators to the pile-groups. Two electro-hydraulic

actuators, elevated 340 and 190 cm above ground level, were used to impose the computed displacement response of the systems taken from a numerical algorithm for the test structures.

In our hybrid analysis, we consider the structural system to be idealized by a sway-rocking model of 2 degrees of freedoms. In the idealization, we replaced the piles by sway and rocking springs and dampers to represent the resistance of the pile foundation to displacement and rotation at its top.

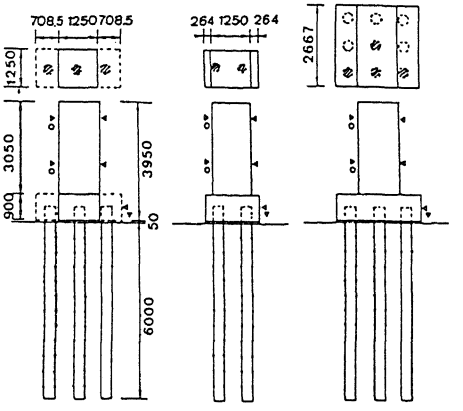


Figure 2. Pile group foundations tested.

Table 1. Mechanical properties of pile foundations

| | 1 pile | 2 piles | 3 piles | 9 piles |
|---|---|---|---|---|
| Upper actuator (cm) | 340 | 340 | 340 | 340 |
| Lower actuator (cm) | 190 | 190 | 190 | 190 |
| Center of gravity (cm) | 197.5 | 184.1 | 166.2 | 166.2 |
| Mass (tonf·s²/cm) | 0.0151 | 0.0166 | 0.0190 | 0.0406 |
| Moment of inertia (tonf·cm·s²) | 215.4 | 256.9 | 329.5 | 704.7 |

Table 2. Mechanical properties of the piles.

| | |
|---|---|
| Modulus of elasticity E (kgf/cm²) | 2.10 x 10⁶ |
| Section second moment of area I (cm⁴) | 1.55 x 10⁴ |
| Embedded length of pile L (m) | 6.0 |
| Area of steel section A (cm²) | 103.3 |
| Weight per unit length w (kgf/m) | 81.0 |
| Diameter D (mm) | 355.6 |
| Thickness t (mm) | 9.5 |

## 2.2 System static and dynamic equilibrium

The experiments consisted of three assays; static, dynamic and pseudo-dynamic testing. In the static tests, the two actuators were synchronized so as to excite the sway and rocking modes independently. The static equilibrium of the system is

$$\begin{Bmatrix} F \\ M \end{Bmatrix} = \begin{bmatrix} k_x & -k_x(h_G-h_S) \\ -k_x(h_G-h_S) & k_\theta+k_x(h_G-h_S)^2 \end{bmatrix} \begin{Bmatrix} x \\ \theta \end{Bmatrix} \quad (1)$$

in which F and M are the exciting force and moment, x and θ the displacement and rotation angle at or around the center of gravity, $k_x$ and $k_\theta$ the stiffnesses of the sway and rocking spring, and $h_G$ and $h_S$ the heights of the gravity point and sway spring.

Six cycles of loading and unloading in 0.5 cm increments from 0.5 to 3 cm maximum displacement amplitudes were conducted in each static test. Secant stiffnesses at each step in the static tests were computed and drawn against their corresponding displacements. Results for all the pile groups are shown in Figure 3.

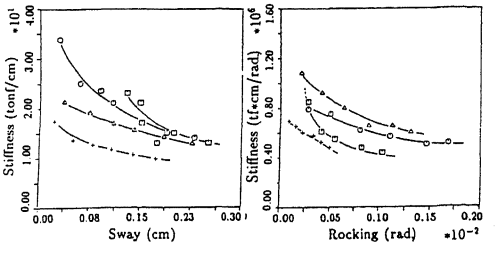


Figure 3. Static test results: Secant modulus at each cycle of the test for the sway (left) and rocking (right) modes. PL1 (square), PL2 (circle), PL3 (triangle) and PL9 (plus)

Dynamic forced vibration tests were made to obtain sufficient data to define three mathematical models of the half-space for use in the soil-structure interaction study. The actuators produced a harmonically varying displacement amplitude of 0.5 mm which excited the foundation into harmonic vibration at the excitation frequency used. During the test the frequency was varied from 0.5 to 12 Hz in 0.5 Hz increments.

The dynamic equilibrium of the system is given as

$$\begin{bmatrix} -\omega^2 M_0+i\omega c_x+k_x & -(i\omega c_x+k_x)h_G \\ -(i\omega c_x+k_x)h_G & -\omega^2 I_0+i\omega(c_\theta+c_x h_G^2)+(k_\theta+k_x h_G^2) \end{bmatrix} \times \begin{Bmatrix} X\exp(-i\phi_x) \\ \Theta\exp(-i\phi_\theta) \end{Bmatrix} = \begin{Bmatrix} F \\ M \end{Bmatrix} \quad (2)$$

in which $c_x$ and $c_\theta$ are the damping coefficients of the sway and rocking motions, X and Θ the amplitudes of the sway displacement and the rotation angle, and $\phi_x$ and $\phi_\theta$ the phase delays.

Dynamic test results are given in Figure 4 in which the amplitude and phase spectra in the sway mode are shown against cyclic frequency. The frequency-dependent stiffness and viscous damping of the soil-pile-foundation system in the sway and rocking modes, obtained from the amplitude and phase shift

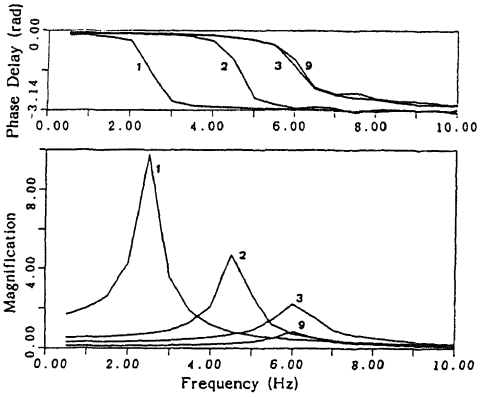


Figure 4. Dynamic test results: Phase (top) and Amplitude (bottom).

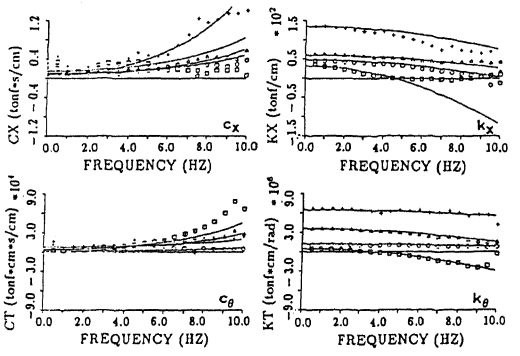


Figure 5. Frequency dependence of dynamic characteristics for stiffness (top) and damping (bottom) in the sway (left) and rocking (right) modes: PL1 (square), PL2 (circle), PL3 (triangle) and PL9 (plus).

study, are shown by symbols in Figure 5. Simplified correlated functions, (shown by solid lines in the figure) were used to construct the soil-foundation interaction models.

For the PFD, we have developed a time-domain integration scheme which gives the frequency dependence of dynamic characteristics through the introduction of a time-history-dependent pseudo-forcing function. In practice, because of the presence of noise and errors in measurements and the approximation and modeling of the frequency-dependent dynamic characteristics, we have to use functions that satisfy causality conditions prior to the inverse transformation. To satisfy these conditions (the imaginary part of the complex stiffness must be identical to the Hilbert Transformation of its real part), we derived a time-dependent dynamic stiffness function which accounts for the frequency dependence in the time domain through a time-dependent function.

For the modelings, the respective equations of motion to be used in the PDT are written in a matrix form as

$$[M]\{\ddot{x}\} + [C_0]\{\dot{x}\} + \{F\} = -[M]\{\ddot{y}\} - \int_0^t [K^*(t-\tau)]\{F(\tau)\}\, d\tau \quad (3)$$

$$\{F\} = [K_0]\{x\} \quad (4)$$

$$[K^*] = [\overline{K^*}][K_0]^{-1} \quad (5)$$

in which [M] is the lumped mass matrix, $[C_0]$ and $[K_0]$ are the constant part of damping and the stiffness matrix, {F} is the restoring force and moment, {x} and {y} are the response and the input vector, and $[\overline{K^*}]$ is the inverse Fourier transform of complex stiffness. The hybrid experiment is done by incorporating {F} from the experiment into equation (3) and is fed-back to the experiment.

Three different accelerograms; Taft (July 21, 1952), Hachinohe (May 16, 1968), and Ibaragi (July 12, 1987 recorded at the site of the experiments) were used in our hybrid study.

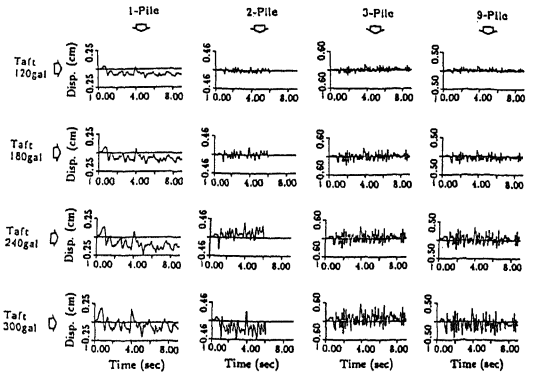


Figure 6 (a). Sway displacement response of PL1, PL2, PL3 and PL9 under Taft with 120 to 300 gals.

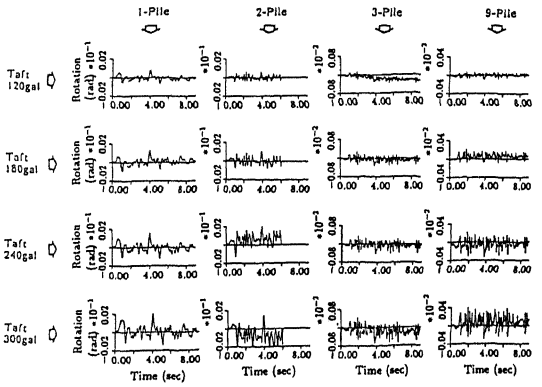


Figure 6 (b). Rocking displacement response of PL1, PL2, PL3 and PL9 under Taft with 120 to 300 gals.

## 2.3 Discussion and results

In a previous study (Toki 1990), we used the same method and procedure with large scale foundation models to investigate the nonlinear seismic behavior of surface, shallow embedded and caisson foundations. This method satisfactorily accounted for the nonlinearity and frequency dependency of the soil-structure system. In that research, we studied the effects of foundation embedment, frequency-dependent modeling, different input wave-forms and amplitude scaling through comparisons of results obtained from static, dynamic and pseudo-dynamic tests. We here report a study on the effects of pile-grouping, frequency-dependent modeling and restoring force hysteresis loops.

Sway and rocking displacement responses of PL1, PL2, PL3 and PL9 are shown in Figure 6 (a), (b) for the Taft input with amplitudes increasing from 120 to 300 gals. As expected, both the maximum response amplitude and the permanent residual displacement increase with input amplitude. This is mainly because the soil around the piles softens and separates under repeated loading with a concomitant decrease in stiffness. For these piles, the measured response peaks shift to lower frequencies and become sharper with load repetition. An increase in the number of piles in a pile group increases rocking stiffness much more than sway; therefore the piles tend to dissipate the input energy by oscillating more in the sway than rocking mode. This phenomenon is explained by the fact that for groups with a large number of piles, the need to satisfy geometrical compatibility at the pile group cap increases system rigidity in the rocking more than in the sway mode.

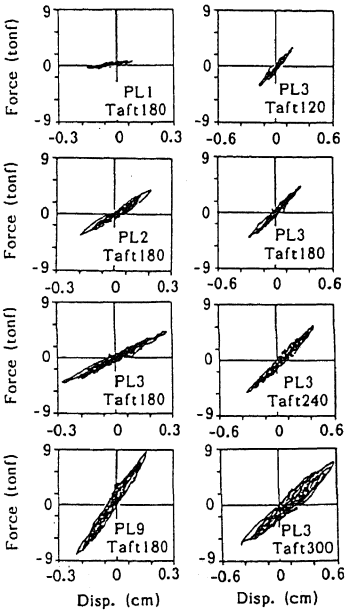


Figure 7. Restoring force hysteresis loops. Left: PL1, PL2, PL3 and PL9, Right: PL3 under Taft with 120 to 300 gals.

Considerable insight into the nature of a nonlinear system is obtainable from knowledge of its generalized restoring force. Figure 7 shows modal restoring force diagrams that have experienced strong shaking. Stiffness reduction with consecutive cycles of response is apparent from these diagrams and is associated with the progressive rotation of the hysteresis loops clockwise. The difference between the initial and final stiffness is a measure of the stiffness lost and is related to the amount of deterioration suffered by the system.

## 3 DEAD LOAD EFFECT ON PILE GROUPS

For piles and pile group design purposes the system's responses in translation and rotation are considered to be independent of axial deformation; i.e., the axial loading of piles has no effect on their sway and rocking characteristics.

To investigate and estimate this coupling and to study the effect of increasing the dead loading on the sway-rocking response of pile foundations, we used the PL3 pile group model. Four dead loadings of 10, 20, 30 and 40 tons were given the PL3 to increase the axial loads on its piles. Dead loads were provided by steel plates placed one at a time on the top portion of the foundation stem. The plates were fixed and tied tightly in place so that they could not produce independent movement and vibration during the static, dynamic and pseudo-dynamic tests (Figure 8).

Following the test set-up, static and forced vibration dynamic tests were conducted, and the mechanical characteristics of the new PL3 with the additional dead loads were determined. The secant static stiffnesses of the PL3 with additional 10, 20, 30 and 40 tons dead

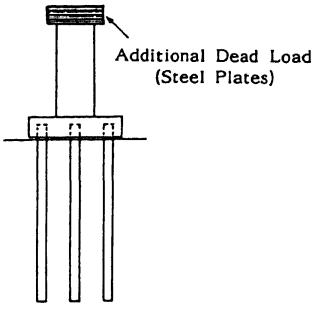


Figure 8. Test set-up for additional dead loading.

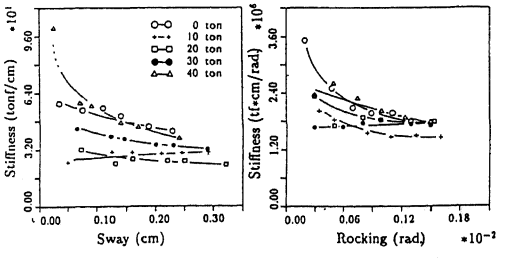


Figure 9. Static secant stiffness of PL3 with additional dead loading.

loads are given in Figure 9. Static stiffness appears to be independent of the additional dead loading, the slopes remaining almost unchanged, especially in the rocking mode.

An additional dead load increases the system's mass and thereby the natural frequency. This behavior is clearly shown in Figure 10 in which results from the forced vibration dynamic tests are given for PL3 with extra dead loadings. The case of PL3 without additional loading is presented for comparison.

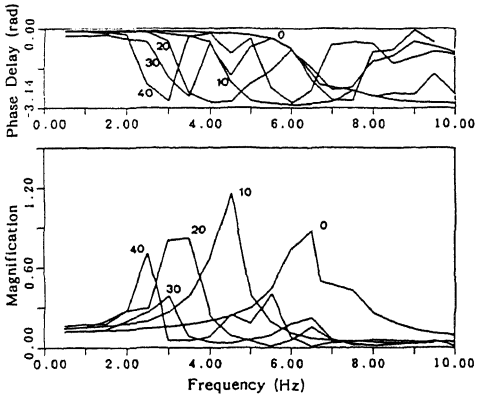


Figure 10. Dynamic test results for PL3 with additional dead loading.

The mechanical characteristics of the PL3 with additional dead loadings determined from the static and dynamic tests were used to construct soil-structure models. Consequently, for each loading case the nonlinear seismic responses of the systems were simulated by the hybrid experiment method and the S69E component of the Taft accelerogram with 180 gals was used for the pseudo-dynamic tests.

The sway and rocking displacements for loadings of 0, 10, 20 and 30 tons (given in Figure 11 for the Taft 180 gals input) show that the additional dead loading increases the response amplitudes in both of the sway and rocking modes, notably for the first added 10 tons. Although additional dead loading, increases the mass of the pile foundation, it has almost no effect on the strength of the system. This produces additional seismic force, thereby increasing the sway and rocking response amplitudes. Consequently, the restoring force and moment response amplitudes increase.

## 4 OBSERVED SEISMIC DATA

Opportunities to observe actual seismic data for PL2 and PL9 were provided when an earthquake took place at the site of our hybrid experiments. The location of the free-field observation and test sites, and the arrangement of seismograms are shown in Figure 12 (a), (b). We made hybrid experiments in which the recorded accelerograms at the free-field site were used as the base excitations. The transfer functions for the observations and experiments are plotted in Figure 13 (a), (b). The transfer function for the recorded data is calculated from the ratio of the East-West component of the response of the foundation and the acceleration

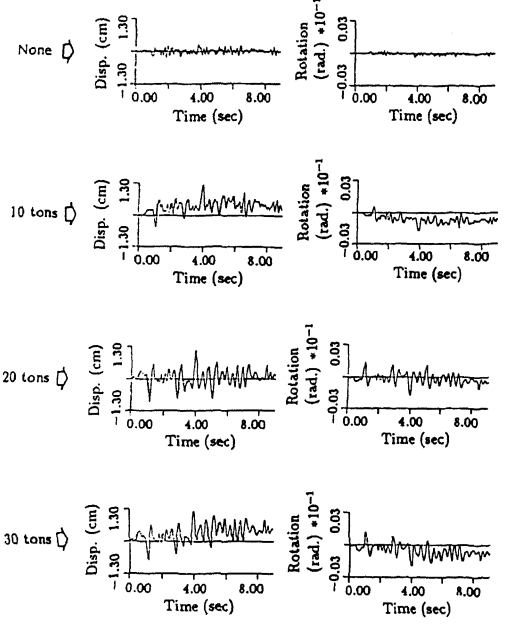


*Figure 11. Sway and rocking displacement for Taft 180 gals input.*

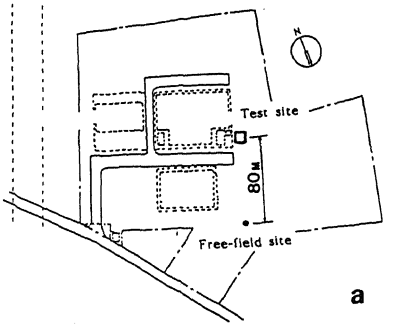


Figure 12 (a). Location of the free-field and test foundation sites.

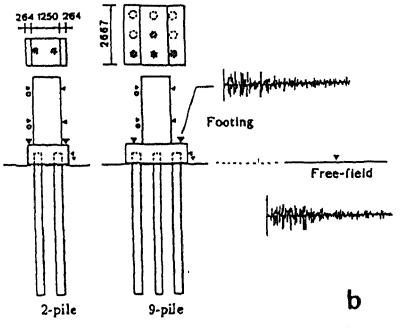


Figure 12 (b). Arrangement of seismograms.

at the free-field. The transfer function for the experiment is given for the ratio of the recorded response of the footing in the experiment and the input excitation. The respective natural frequencies of the first mode of PL2 and PL9 are 4.5 and 6 Hz. The figures show that the transfer functions based on the experiments (PL2, PL9; 120, 240 and 360 gals) are very similar except in the long period range. Unlike in the experimental functions, high frequency components are lacking in the observed functions. These phenomena suggest that the free-field motion as input motion is effected by the kinematic interaction. The transfer functions of PL9 calculated from two sets of earthquake data are shown in Figure 14. The peak accelerations for the free-field are 5 and 30 gals.

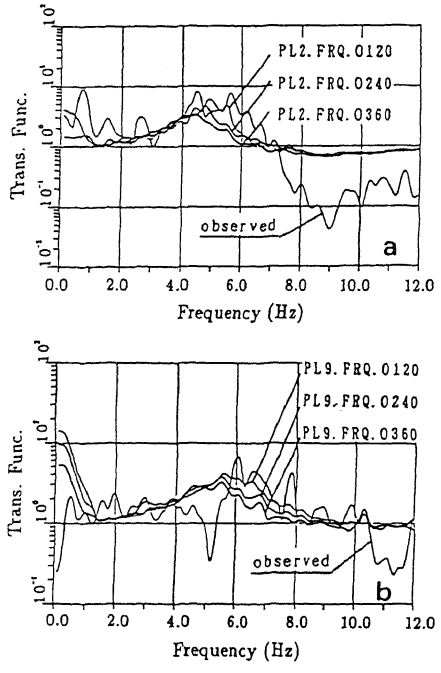


Figure 13. Comparison of transfer functions for recorded observations and experiments: (a) PL2, (b) PL9

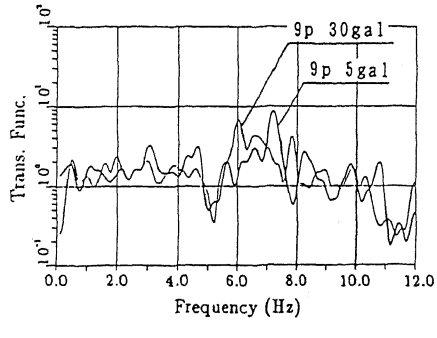


Figure 14. Comparison of the transfer functions of PL9

Although the shapes of the functions are similar, the predominant frequency of the larger amplitude event is in the longer period range. This availability of recorded seismic data for a pile group foundation made it possible to evaluate the frequency-dependent, soil-structure interaction model used in our hybrid experiments.

## 5 CONCLUSIONS

We conclude that, hybrid experiments made on soil-structure systems provide an efficient and versatile tool with which to determine the material and geometrical nonlinearities of soil-structure systems that occur during strong ground motion.

Four dead loadings of 10, 20, 30 and 40 tons were used with the PL3 group model to increase the axial loads on the piles in order to investigate the effect of increased dead loading on the sway-rocking response of pile foundations. Although additional dead loading increases the mass of the pile foundation, it has almost no effect on the strength of the system.

Although the transfer functions for recorded observations and the experiment are in good agreement, the lack of high frequency components in the transfer function for the observations suggests that as the input motion of the experiment, input excitation through the kinematic interaction is preferable.

## ACKNOWLEDGEMENTS

This study was supported by a grant from the Ministry of Education, Science and Culture of Japan, (No.62850085) and in part by the Hanshin Expressway Public Corporation. It was conducted under a joint-research program sponsored by the Disaster Prevention Research Institute of Kyoto University and the Tsukuba Research Institute of Okumura Corp. We also gratefully acknowledge the contributions of our co-workers Prof. T. Sato, Dr. N. Kishi Garmroudi, Dr. S. Emi, Dr. M. Yoshikawa and Mr. T. Arano.

## REFEREFCES

Papoulis, A. 1962. The Fourier integral and its applications. London: McGraw-Hill.

Toki, K., T. Sato, J. Kiyono, N. Kishi G. & M. Yoshikawa, 1988. Development of a hybrid experiment method for nonlinear soil-structure interaction systems. Annals of the Disaster Prevention Research Institute, Kyoto University, No.31B-2 : 23-38. (in Japanese).

Toki, K., T. Sato, J. Kiyono, N. Kishi Garmroudi, S. Emi & M. Yoshikawa 1990. Hybrid experiments on nonlinear earthquake-induced soil-structure interaction, International Journal of Earthquake Engineering and Structural Dynamics, Vol. 19, No. 6 : 709-723.

Veletsos, A.S., A. M. Prasad and Y. Tang 1988. Design approaches for soil-structure interaction, NCEER-88-0031. Buffalo: State University of New York.